

Water in the lunar interior

A. Basu Sarbadhikari, K. K. Marhas, Sameer and J. N. Goswami*

Physical Research Laboratory, Ahmedabad 380 009, India

Presence and distribution of water and other volatiles in the lunar interior could have played a key role in the early evolution of the Moon. We report abundance of water along with F and Cl, in apatite present in the Apollo 15 lunar basalt 15555, considered to be the primitive end member of the low-Ti mare basalt suite. Apatites are rare in this basalt and are devoid of significant spatial variation in volatile content. Considering a late-stage crystallization of apatite, we infer 100–160 ppm water, 80–90 ppm fluorine and 10–20 ppm chlorine in the parent magma of 15555. The inferred water content is much lower than that reported for the parent magma of lunar volcanic glasses, as well as in melt inclusions trapped within the glasses that sampled much deeper regions of Moon. This difference suggests a non-uniform distribution of water and other volatiles in lunar mantle source regions, that could have significantly influenced early thermochemical evolution of the Moon.

Keywords: Apatite, lunar interior, mare basalt, moon, water.

WIDESPREAD presence of surface-cited water as well as evidence for the presence of subsurface water ice in the lunar polar regions^{1–3} have established that Moon is not bone dry as hypothesized earlier. First signatures for presence of water intrinsic to the Moon came from studies of lunar volcanic glasses collected at the Apollo 15 and 17 landing sites⁴. This together with reports of indigenous volatiles in lunar apatite^{5–10} and in olivine hosted melt inclusions within Apollo 17 volcanic glasses¹¹, suggest that the volatiles in lunar interior could have influenced the lunar magmatic processes. Presence of water could also lead to lowering of viscosity in the lunar mantle. Water intrinsic to the Moon has also been inferred from studies of laboratory reflectance spectra of lunar anorthosites¹² and Chandrayaan-1 spectral reflectance data for different regions on the Moon^{13,14}.

The Apollo 15 and Apollo 17 volcanic glasses contained 4–46 ppm of water⁴. A value of 745 ppm was estimated for the pre-eruptive water content, taking into account diffusive degassing and subsequent glass formation⁴. Olivine hosted melt inclusions in Apollo 17 volcanic glasses contain 615–1410 ppm of water, 50–78 ppm of F and 1.5–3.0 ppm of Cl (ref. 11). High pressure-temperature experimental petrology coupled with geochemical studies^{15,16} suggests a deep mantle source

(≥ 500 km) for the Apollo 15 and 17 volcanic glasses. Apatites in lunar basalts belonging to low-Ti, high-Ti and high-Al groups, also host water over a wide range from few hundreds to several thousands of ppm^{5–10}. These studies suggest water content ranging from 70 to 240 ppm in the parent magmas of lunar basalts. However, a recent study¹⁷ outlined problems associated with accurately retrieving volatile content in melts due to compatible behaviour of fluorine in apatite, that can lead to significant volatile zoning.

In this study, we report the identification of lunar apatite devoid of significant volatile zoning in mare basalt 15555, a slowly cooled microgabbro. This basalt, considered to be the primitive end member of the low-Ti mare basalt suite¹⁸, is composed of olivine, pyroxene, plagioclase and accessory phases, such as tridymite, ilmenite, chromite, ulvöspinel, troilite, glass, Fe–Ni metal and small fluorapatite grains^{18,19}, and have a crystallization age of ~3.3 Ga (ref. 20). High-pressure experiments together with geochemical characteristics of 15555 indicate co-saturation of olivine-orthopyroxene-spinel in the parent magma, at ~8.5 kbar pressure, i.e. 150–200 km below the lunar surface, in a closed system¹⁸.

A polished thick section of the lunar basalt 15555 was analysed in this study. Apatite generally occurs in association with clinopyroxene, plagioclase, silica, ilmenite and glass, and was identified by taking back-scattered electron and X-ray elemental (Ca, P) images with a Cameca SX-100 electron microprobe. Two relatively large apatite grains (B1: ~30 µm and B2: ~20 µm) were selected for this study (Figure 1).

A Cameca secondary ion mass spectrometer (nano-SIMS50) was used to analyse the apatite grains for their volatile composition. The thick section of 15555 was repolished to remove a few micron layers to conduct isotope studies on fresh surfaces of apatite. Each grain and its surrounding areas were extensively pre-sputtered with a high intensity (~1 nA) Cs⁺ beam for 15–20 min, to expose clean, pristine grain surfaces. A 16 KeV Cs⁺ primary beam of ~50 pA and diameter 0.5 µm was used to raster 40 µm × 40 µm area covering the apatite grain surface. Pressure in the analysis chamber was maintained at ~10⁻¹⁰ torr to minimize OH⁻ background. Secondary ions, ¹⁶O¹H⁻, ¹⁸O⁻, ¹⁹F⁻, ³¹P⁻ and ³⁵Cl⁻, were collected simultaneously using five different electron multipliers. Magnetic field stability was controlled using an NMR probe that ensured minimal field drift (~10 ppm) during analyses. The mass resolution M/ΔM of ~4000 used for the analyses cannot fully resolve the ¹⁶O¹H and the ¹⁷O flat-top peaks. The ¹⁶O¹H⁻ ions were collected with a small mass offset to ensure contribution from the ¹⁷O⁻ peak is less than a few percent. Data were acquired in both 'isotope (ion count rate)' and 'image' modes, for each of the 50 raster scans performed during a typical analysis that lasted about an hour. Durango apatite was used as a standard for inferring volatile content in the

*For correspondence. (e-mail: goswami@prl.res.in)

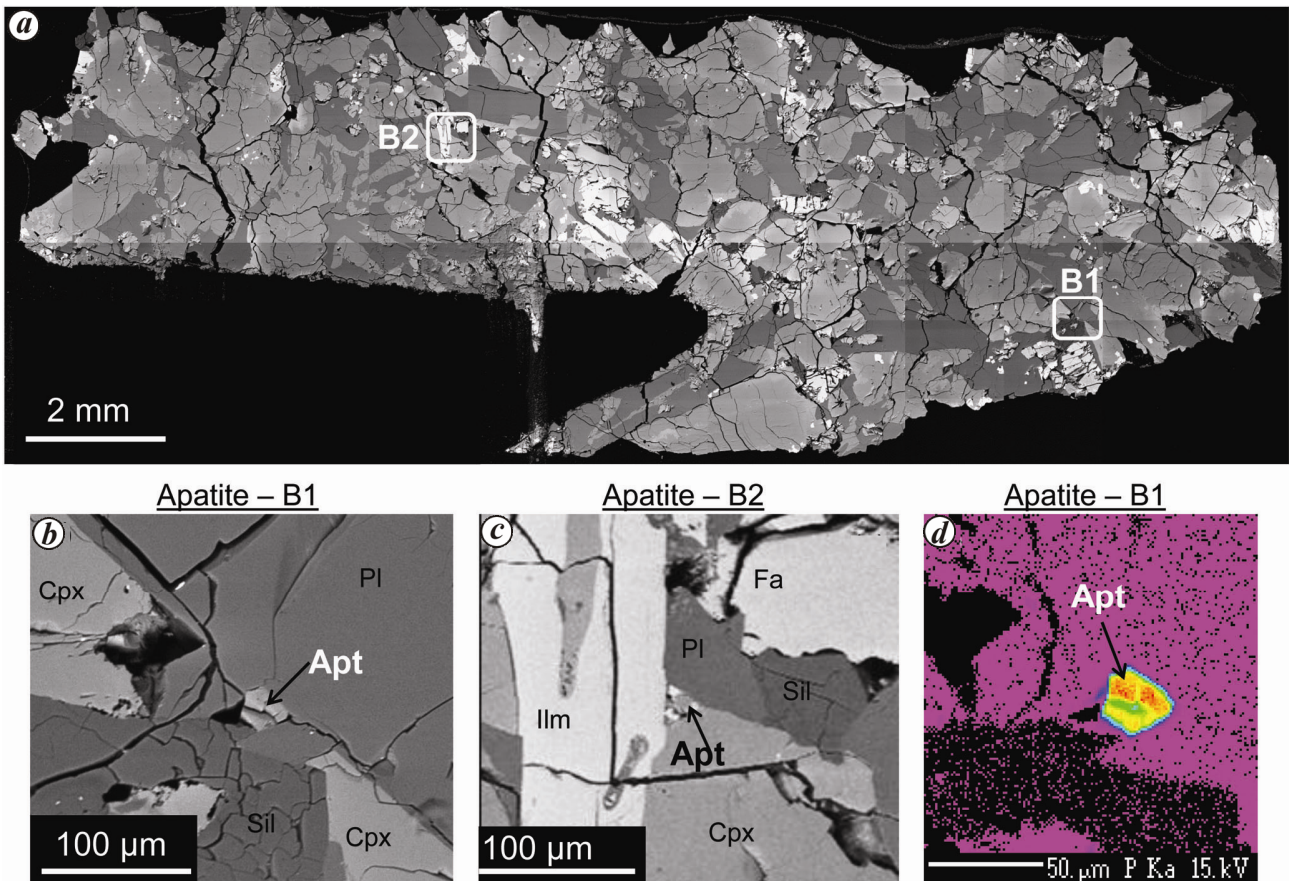


Figure 1. Back-scattered electron images of a section of 15555 mare basalt (*a*), and apatite grains B1 (*b*) and B2 (*c*), along with phosphorus X-ray image of apatite B1 (*d*). Mineral abbreviations are: Fa, fayalitic olivine; Cpx, clinopyroxene; Pl, plagioclase; Sil, silica; Ilm, ilmenite; Apt, apatite.

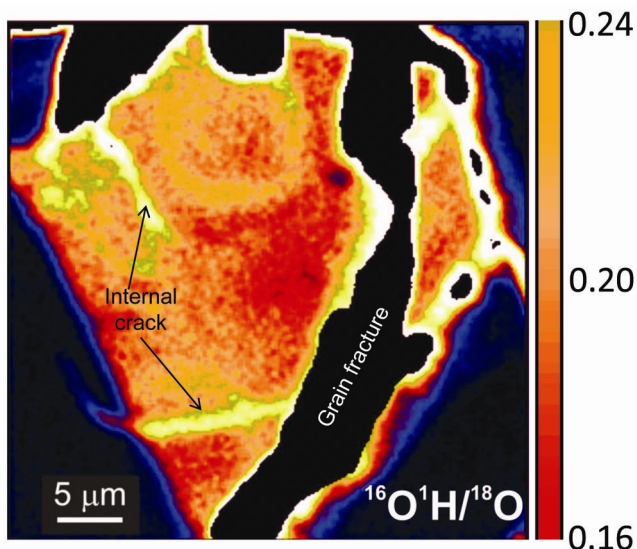


Figure 2. Colour coded ratio of $^{16}\text{O}^1\text{H}$ counts to that of ^{18}O for the apatite grain B1. Apparent higher values for prominent and small internal fractures as well as for minor cracks and grain boundaries (shades of white, green and light yellow) are artefacts. No systematic spatial variation of water and other volatile content, suggestive of distinct zoning, is apparent.

lunar apatite and was analysed in both ‘imaging’ and ‘isotope’ modes, bracketing the analysis of lunar apatite, to check reproducibility as well as correlation between the two modes of analysis.

The NanoSIMS data obtained in the imaging mode were reduced using a custom software package (L’image, provided by L. Nittler, and Carnegie Institution of Washington). Before the analysis, data from individual image (raster scans) were dead time corrected and aligned with each other to take into account any stage and/or beam drift during analysis. We analysed data from specific regions of interest in each lunar apatite, away from fractures, cracks and grain boundaries. Water content in the two apatite grains ranges from 2200 to 2850 ppm (apatite B1; Figure 2) and 3400 to 3750 ppm (apatite B2). Abundances of fluorine in the two grains are 2.7–3.1 wt% (B1) and 2.7–2.8 wt% (B2). The values for chlorine content are 0.14–0.15 wt% (B1) and 0.085–0.125 wt% (B2).

A recent study¹⁷ pointed out that the simplified approach used in previous studies of lunar apatite for inferring lunar volatile content may not be exact as the volatiles OH, F and Cl prefer specific site occupancy rather than behaving like incompatible elements during

apatite crystallization. In such a case, one expects systematic spatial variation of volatile content in individual apatite grains from core to rim and this was indeed seen in large (100–400 μm) lunar apatites^{6,7}. Even though minor variation in water content is present in the two small apatite grains from 15555, there is no discernible trend suggestive of volatile compositional gradation or zoning (Figure 2). The dark red patches, present inconsistently from centre to near the edge of the apatite grain, host water in the range of 2200–2450 ppm, and the yellowish-red regions represent water content of 2500–2850 ppm. The distributions of Cl and F in this apatite are also not suggestive of compositional zoning. The apparent high water contents in this apatite in some narrow zones are not intrinsic and are artefacts due to the presence of internal cracks and/or grain edges. The nearly uniform distribution of volatiles in the two grains makes it highly unlikely that this could result from preferred site-occupancy or exchange equilibration, and suggest that the volatiles entered into apatite structure guided primarily by their respective partition coefficients.

Partition coefficients of F and Cl between apatite and basaltic melt are available from experimental study²¹ and are 3.4 (F) and 0.8 (Cl) respectively. Even though partition coefficient of water between apatite and basaltic melt was not explicitly mentioned, one can infer these values from the same dataset²¹. We considered the range of water content in 15555 apatite, from 0.2 to 0.7 wt%¹⁰ (this study), and also data reported for other mare basalts (up to 1.5 wt%)^{5–10} and obtained partition coefficient of water between apatite and basaltic melt ranging from 0.05 to 0.23. An upper limit of 0.3 has also been suggested based on data obtained in a recent experiment²². In the absence of experimentally-derived thermodynamic dataset of lunar apatite, a direct assessment of their stage of crystallization is difficult. We assume 99% crystallization stage of apatite in 15555, based on values suggested by Tartèse *et al.*¹⁰, and consider the upper limit of partition coefficient from laboratory data (0.23), and infer values of 100–160 ppm of water, 80–90 ppm of F and 10–20 ppm of Cl in the parent magma of lunar mare basalt 15555.

Studies of Apollo 15 and Apollo 17 lunar volcanic glasses, that sampled a deeper region (≥ 500 km)^{15,16} of the lunar interior, relative to the mare basalts, yielded a value of 745 ppm for the abundance of water in the parent magmas of these lunar volcanic glasses⁴. Melt inclusions trapped in Apollo 17 volcanic glasses yielded water content in the range of 615–1410 ppm (ref. 11). These values are much higher than those for the parent magmas of the Apollo 15 mare basalt 15555 that originated at a depth of 150–200 km below the lunar surface¹⁸. This suggests a non-uniform distribution of water and other volatiles in the lunar interior. This needs to be taken into account in any estimation of the bulk water content of Moon. Presence of water in lunar mantle could have significantly

affected the early evolution of Moon and in particular, helped in sustaining a lunar core dynamo for an extended duration²³. High water content would also lower the solidus–liquidus temperature of the deeper mantle source of volcanic glasses in comparison to the upper mantle source of the mare basalts. This can influence a change in thermo-chemical processes, e.g. differential degree of melting, in different mantle source regions during the early evolutionary stages of the Moon. Further studies of melt inclusions trapped in lunar volcanic glasses and in lunar basalts are needed for a better understanding of the distribution of volatiles in the lunar interior.

- Pieters, C. M. *et al.*, Character and spatial distribution of OH/H₂O on the surface of the Moon seen by M³ on Chandrayaan-1. *Science*, 2009, **326**, 568–572.
- Spudis, P. D. *et al.*, Initial results for the North Pole of the Moon from Mini-SAR, Chandrayaan-1 mission. *Geophys. Res. Lett.*, 2010, **37**, L06204.
- Colaprete, A. *et al.*, Detection of water in the LCROSS Ejecta Plume. *Science*, 2010, **330**, 463–468.
- Saal, A. E., Hauri, E. H., Cascio, M. L., Van Orman, J. A., Rutherford, M. C. and Cooper, R. F., Volatile content of lunar volcanic glasses and the presence of water in the Moon's interior. *Nature*, 2008, **454**, 192–196.
- Boyce, J. W., Liu, Y., Rossman, G. R., Guan, Y., Eiler, J. M., Stolper, E. M. and Taylor, L. A., Lunar apatite with terrestrial volatile abundances. *Nature*, 2010, **466**, 466–469.
- McCubbin, F. M., Steele, A., Hauri, E. H., Nekvasil, H., Yamashita, S. and Hemley, R. J., Nominally hydrous magmatism on the Moon. *Proc. Natl. Acad. Sci. USA*, 2010, **107**, 11223–11228.
- Greenwood, J. P., Itoh, S., Sakamoto, N., Warren, P., Taylor, L. and Yurimoto, H., Hydrogen isotope ratios in lunar rocks indicate delivery of cometary water to the moon. *Nature Geosci.*, 2011, **4**, 79–82.
- Basu Sarbadhikari, A., Marhas, K. K., Sameer, Goswami, J. N., Water content in melt inclusions and apatites in low-titanium lunar mare basalt, 15555. In Lunar and Planetary Science Conference, Texas, 2013, vol. 44, Abstr. 2813.
- Tartèse, R. and Anand, M., Late delivery of chondritic hydrogen into the lunar mantle: insights from mare basalts. *Earth Planet. Sci. Lett.*, 2013, **361**, 480–486.
- Tartèse, R., Anand, M., Barnes, J. J., Starkey, N. A., Franchi, I. A. and Sano, Y., The abundance, distribution, and isotopic composition of hydrogen in the moon as revealed by basaltic lunar samples: Implications for the volatile inventory of the moon. *Geochim. Cosmochim. Acta*, 2013, **122**, 58–74.
- Hauri, E. H., Weinreich, T., Saal, A. E., Rutherford, M. C. and Van Orman, J. A., High pre-eruptive water contents preserved in lunar melt inclusions. *Science*, 2011, **333**, 213–215.
- Hui, H., Peslier, A. H., Zhang, Y. and Neal, C. R., Water in lunar anorthosites and evidence for a wet early Moon. *Nature Geosci.*, 2013, **6**, 177–180.
- Bhattacharya, S., Saran, S., Dagar, A., Chauhan, P., Chauhan, M., Ajai and Kiran Kumar, A. S., Endogenic water on the Moon associated with non-mare silicic volcanism: implications for hydrated lunar interior. *Curr. Sci.*, 2013, **105**, 685–691.
- Klima, R. L., Cahill, J., Hagerty, J. and Lawrence, D., Remote detection of magmatic water in Bullialdus Crater on the Moon. *Nature Geosci.*, 2013, **6**, 737–741.
- Delano, J. W., Chemistry and liquidus phase relations of Apollo 15 red glass: Implications for the deep lunar interior. *Proc. Lunar Planet Sci. Conf.*, 1980, **11**, 251–288.

16. Longhi, J., Experimental petrology and petrogenesis of mare volcanics. *Geochim. Cosmochim. Acta*, 1992, **56**, 2235–2251.
17. Boyce, J. W., Tomlinson, S. M., McCubbin, F. M., Greenwood, J. P. and Treiman, A. H., The Lunar Apatite Paradox. *Science*, 2014, **344**, 400–402.
18. Walker, D., Longhi, J., Lasaga, A. C., Stolper, E. M., Grove, T. L. and Hays, J. F., Slowly cooled microgabbros 15555 and 15056. *Proc. Lunar Sci. Conf.*, 1977, **8**, 1521–1547.
19. 15555 Olivine-normative Basalt. In Lunar Sample Compendium. Astromaterials Research and Exploration Science (ARES), Johnson Space Center, Houston, Texas, 2010.
20. Papanastassiou, D. A. and Wasserburg, G. J., Rb-Sr ages and initial strontium in basalts from Apollo 15. *Earth Planet. Sci. Lett.*, 1973, **17**, 324–337.
21. Mathez, E. and Webster, J., Partitioning behaviour of chlorine and fluorine in the system apatite-silicate melt-fluid. *Geochim. Cosmochim. Acta*, 2005, **69**, 1275–1286.
22. Vander Kaaden, K. E., McCubbin, F. M., Whitson, E. S., Hauri, E. H. and Wang, J., Partitioning of F, Cl, and H₂O between apatite and a synthetic shergottite liquid (QUE 94201) at 1.0 GPa and 990–1000°C. In *Lunar and Planetary Science Conference*, Texas, 2012, vol. 43, Abstr. 1247.
23. Evans, A. J., Zuber, M. T., Weiss, B. P. and Tikoo, S. M., A wet, heterogeneous lunar interior: Lower mantle and core dynamo evolution. *J. Geophys. Res.: Planets*, 2014, **119**, doi: 10.1002/2013JE004494.

ACKNOWLEDGEMENTS. We thank the anonymous reviewers for constructive comments and Francis McCubbin of University of New Mexico for providing the Durango apatite standard. We acknowledge support provided by Dipak Panda and Lalit Shukla during EPMA and NanoSIMS analysis respectively.

Received 6 January 2015; revised accepted 17 December 2015

doi: 10.18520/cs/v110/i8/1536-1539

Carbon isotopic composition of suspended particulate matter and dissolved inorganic carbon in the Cochin estuary during post-monsoon

P. S. Bhavya^{1*}, Sanjeev Kumar^{1*},
G. V. M. Gupta², K. V. Sudharma², V. Sudheesh²
and K. R. Dhanya²

¹Physical Research Laboratory, Navrangpura,
Ahmedabad 380 009, India

²Centre for Marine Living Resources and Ecology,
Ministry of Earth Sciences, Kendriya Bhavan, Cochin 682 037, India

Detailed measurements of carbon (C) isotopic composition in dissolved inorganic ($\delta^{13}\text{C}_{\text{DIC}}$) and particulate organic ($\delta^{13}\text{C}_{\text{POC}}$) fractions were conducted at 18 stations in the Cochin estuary during the post-monsoon season. In general, C biogeochemistry of different regions of the Cochin estuary appears to be regulated by different sources and processes. The northern zone of the estuary appears to be influenced primarily by

mixing of sea water enriched in $^{13}\text{C}_{\text{POC}}$ and $^{13}\text{C}_{\text{DIC}}$, and river run-off depleted in the same. In contrast, the southern zone of the estuary was found to be greatly influenced by local terrestrial sources. Relatively depleted $^{13}\text{C}_{\text{POC}}$ in the freshwater Vembanad lake compared to the main estuary suggests inputs from terrestrial sources along with *in situ* productivity.

Keywords: Carbon isotopic composition, estuary, particulate organic matter, terrestrial sources.

ESTUARIES and lakes are emerging as prominent sources of CO₂ (refs 1–7), globally as they are estimated to emit 0.43 Pg C y⁻¹ and 0.14 Pg C y⁻¹ respectively^{8,9}. An updated estimate shows that inner estuaries, salt marshes and mangroves around the world¹⁰ emit ~0.50 Pg C y⁻¹, while Indian estuaries¹¹ emit 1.92 Tg C y⁻¹. Estuaries which are in contact with large human settlements sustain high rates of CO₂ emission^{6,12–15} due to enhanced mineralization of river-borne particulate organic matter (POM) and heterotrophy^{1,3}. The sources of POM in the estuaries are both allochthonous and autochthonous. Allochthonous sources include terrestrial organic matter (TOM), domestic and industrial run-off, and marine inputs, whereas autochthonous sources comprise materials from estuarine sources. Consequently, the dissolved inorganic carbon (DIC) pool in estuaries also gets amended by both these influences. It is thus important to understand the sources and pathways of POM to decipher its role in carbon (C), nitrogen (N) and oxygen (O) cycles within estuaries and coastal areas, and its overall importance in the global C cycle¹⁶.

Although several studies have been conducted on plankton dynamics and POM in estuaries around the world^{17–20}, a full understanding of the sources, fate and transformations of POM in tropical estuarine systems is lacking. Previous studies in Indian estuaries have mainly focused on nutrients biogeochemistry, plankton dynamics, trophic status, CO₂ flux, etc. with the exception of some studies related to C isotopic composition of DIC and POM^{4,21,22}. Since isotopic fractionation occurring during each step of C cycling leaves the substrate and product pools with distinguishable isotopic ratio, the stable C isotopic compositions of POM ($\delta^{13}\text{C}_{\text{POC}}$) and DIC ($\delta^{13}\text{C}_{\text{DIC}}$) can be used as proxy to understand various sources and related biogeochemical processes in the C cycle.

The present study provides detailed measurements of $\delta^{13}\text{C}_{\text{POC}}$ and $\delta^{13}\text{C}_{\text{DIC}}$ in the Cochin estuary, one of the important estuaries in India, situated at the interface of the southeastern Arabian Sea and major river systems. The total annual freshwater input to this estuary is about 20,000 Mm³, making it the largest wetland along the west coast of India²³. The seasonal variability and tidal fluctuations in the estuarine salinity play a significant role in the biogeochemistry of this backwater ecosystem²⁴. The Cochin estuary is a pivot for plethora of TOM and conse-

*For correspondence. (e-mail: bhavya@prl.res.in; sanjeev@prl.res.in)